THE JOURNAL OF PHYSICAL CHEMISTRY A

Article

pubs.acs.org/JPCA

Gas-Phase Electronic Transitions of $C_{17}H_{12}N^+$ at 15 K

F.-X. Hardy, C. A. Rice, O. Gause, and J. P. Maier*

Department of Chemistry, University of Basel, Klingelbergstrasse 80, CH-4056 Basel, Switzerland

ABSTRACT: The electronic spectrum of $C_{17}H_{12}N^+$, phenanthrene with a side chain, was measured in the gas phase at a vibrational and rotational temperature of ~15 K in an ion trap using a resonant multiphoton dissociation technique. The $C_{17}H_{12}N^+$ structure was produced in a chemical ionization source and identified by a comparison with theoretical calculations of stable structures and excitation energies. The (3), (2), (1) $^1A \leftarrow X\ ^1A$ electronic transitions of this nitrogen-containing aromatic species with 30 atoms have origin band maxima at 23 586 ± 1 cm^{-1}, 16 120 ± 50 cm^{-1}, and 14 519 ± 30 cm^{-1}. Distinct vibrational structure in the (3) ^1A state is observed, and assignments are made. Astronomical aspects are considered.

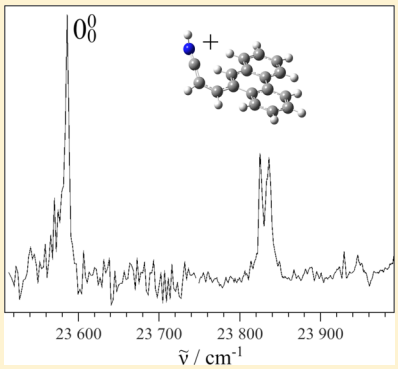

1. INTRODUCTION

A challenge in molecular spectroscopy is the measurement of electronic spectra of large molecules, including cations, in the gas phase and at low temperatures, where all internal degrees are relaxed to the ground state. Direct absorption methods have the problem that high densities are needed and spectral congestion due to overlapping absorbing species occurs. Laser-induced fluorescence, which is more sensitive, is limited to species that have a detectable quantum yield. In the case of cations, a viable approach is to store them in a radio frequency (rf) trap, relax the vibrations and rotations to a temperature of ~15 K by collisions with cold helium, and to record electronic spectra by resonance-enhanced or multiphoton dissociation (MPD).[1] This technique allows the detection of mass-selected photofragments as a function of laser wavelength, removing any ambiguity in the identity of the ion of interest. However, different isomers of the same m/z cannot be excluded, and spectral signatures assist in the assignment of confined ions.

Polycyclic aromatic hydrocarbons (PAHs) composed of fused benzene rings are proposed to be present within the interstellar medium (ISM).[2,3] They can be ionized by the radiation field and redistribute excess energy efficiently throughout the internal degrees of freedom without causing fragmentation.[3] Ionized PAHs can interact with atomic H or H_2 within interstellar clouds, leading to the formation of protonated PAHs (H^+PAHs), which have been also of interest in the astronomical community because of their possible role as carriers of the unidentified infrared emission bands (UIRs) and diffuse interstellar bands (DIBs).[4−6] Some PAH^+ and H^+PAH have been studied in the gas phase, employing one photon from an infrared, visible, or ultraviolet laser by predissociation of a rare-gas atom.[7] Other gas-phase methods have used MPD using high-power IR radiation or in the visible with lasers.[8,9] Gas-phase electronic spectra of protonated pyrene and coronene measured recently in an ion trap at ~15 K have been compared to known DIB absorptions; however, no matches were found with these species, implying that H^+PAHs even of this size are unlikely to be carriers.[10,11]

Another class of H^+PAHs are protonated nitrogen-containing aromatic systems (H^+PANHs). Nitrogen is the seventh most abundant element in the universe, and it has been proposed that PANHs and H^+PANHs could also be present in the ISM.[3] These sorts of molecules are interesting from an astrobiological perspective because they could have an involvement in prebiotic chemistry and eventual transformation into heterocycles, essential ingredients in biomolecules. This has motivated several gas-phase spectroscopic and theoretical studies of such species.[12−21]

The goal of the present experiment is to measure the electronic spectrum of a larger nitrogen-containing PAH^+ species with both the rotational and vibrational degrees of freedom relaxed by collisions to low temperatures, 10−50 K, as pertinent to the ISM. Therefore, mass-selected ions are introduced into a 22-pole rf trap, where they are brought to ~15 K by collisions with cryogenically cooled helium gas.[10,11] The electronic absorption is measured using tunable laser excitation, and the process is detected by the production of fragment ions in MPD. Electronic transitions of the first three excited states of $C_{17}H_{12}N^+$ (cyanoethyl-substituted phenanthrene), lying in the visible, could be recorded in the gas phase.

2. EXPERIMENTAL METHOD

In Figure 1, the major components of the setup are indicated, the chemical ionization (CI) source, room-temperature hexapole, mass-selected ion injection into a cryogenic rf trap, and

Special Issue: 25th Austin Symposium on Molecular Structure and Dynamics

Received: July 29, 2014
Revised: September 29, 2014

   dx.doi.org/10.1021/jp507616k | J. Phys. Chem. A XXXX, XXX, XXX−XXX

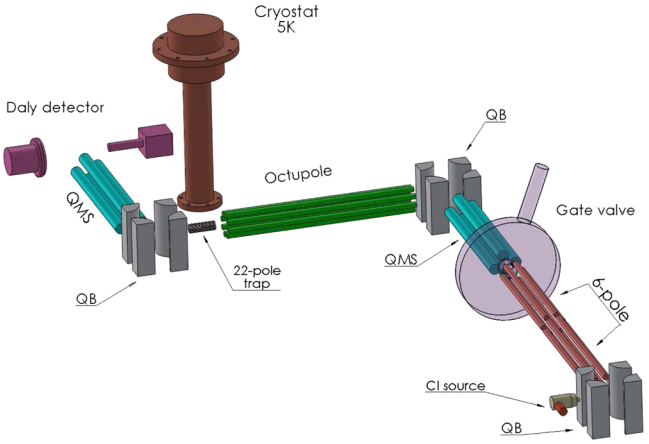

Figure 1. Schematic of the apparatus to record electronic spectra of mass-selected cations at ~15 K. QB is a quadrupole bender and QMS a mass spectrometer.

detection. All ion optics are housed in vacuum chambers, which are divided into six differentially pumped stages.

The substituted phenanthrene was generated by heating a solid sample of 1-azatriphenylene ($C_{17}H_{11}N$) to ~340 K, followed by bombardment of the vapor with 35−40 eV electrons in the presence of toluene in a CI source. The proton affinities of C_7H_8 and $C_{17}H_{11}N$ differ by >130 kJ mol^{-1}, such that the protonation reaction $C_7H_9^+ + C_{17}H_{11}N \rightarrow C_{17}H_{12}N^+ + C_7H_8$ is exothermic. Protonated toluene $C_7H_9^+$ and a plethora of fragment ions were produced in a CI source. Via ion-neutral reactions, $C_7H_9^+$ and other protonated species were created.

Ions are injected through a 2.5 mm electrode into a 440 mm long hexapole (6-pole) divided in two (Figure 1). The applied oscillating rf field has an amplitude of 60−120 V and a frequency of 3.5 MHz and is biased to +8 V. The first six-pole is filled with ~10^{-2} mbar of helium at room temperature, precooling energetic ions from the source. Positive species are confined within the second six-pole and additionally cooled for 50 ms; therefore, the kinetic energy distribution of cations from the source is narrowed. After 50 ms of storage, the exit electrode is lowered by 2.5 V, and ions are released into a quadrupole mass selector (QMS) separated by a gate valve from the rest of the apparatus. The first QMS selects the protonated species with a resolution of ±0.5 au. The ion beam is turned 90° by a quadrupole deflector (QB), injected into an rf-only octupole ion guide and then transported to a 22-pole trap.

A (36 × 10) mm^2 22-pole trap with a radial oscillating field of 7.4 MHz and 80 V amplitude was filled with ~10^5 ions per cycle.[22] The sequence was 40 ms for filling the trap and then 50 ms confinement, followed by laser irradiation and the release of the ions for detection of photoproducts. The 22-pole was mounted on the second stage of a closed-cycle cryostat achieving 5 K. Helium buffer gas was leaked into the trap via a piezovalve,[23] resonating at 3 kHz and 7 V amplitude. A density of ~4 × 10^{15} cm^{-3} was achieved after a few ms, corresponding to approximately one collision per microsecond.

After exiting the trap, ions were collimated by several electrodes and deflected 90° by a QB into the second QMS. The latter selected $C_{17}H_{11}N^+$ fragments, products of the MPD. The ion beam was then focused by an einzel lens and counted by a Daly detector. The experiment was synchronized with a dye laser at a repetition rate of 10 Hz.

Ions were probed by a 5 ns laser pulse via a 1 + 1 excitation−dissociation process. The first photon was resonant with an excited electronic state, and the second promoted $C_{17}H_{12}N^+$ above the fragmentation threshold for the loss of a H atom. The products were selected by the second QMS and counted while varying the wavelength of the laser. A Nd^{3+}:YAG pumped, double grating dye laser (0.07 cm^{-1} bandwidth with ~3−8 mJ energy per pulse) was used to obtain the electronic spectrum of the (3), (2), and (1) $^1A \leftarrow X\ ^1A$ transitions of $C_{17}H_{12}N^+$ (Figures 2 and 3).

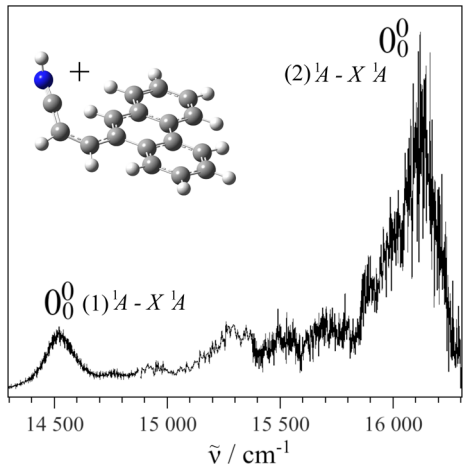

Figure 2. (1) $^1A \leftarrow X\ ^1A$ and (2) $^1A \leftarrow X\ ^1A$ electronic transitions of $C_{17}H_{12}N^+$ measured using a MPD technique with a 0.07 cm^{-1} bandwidth laser.

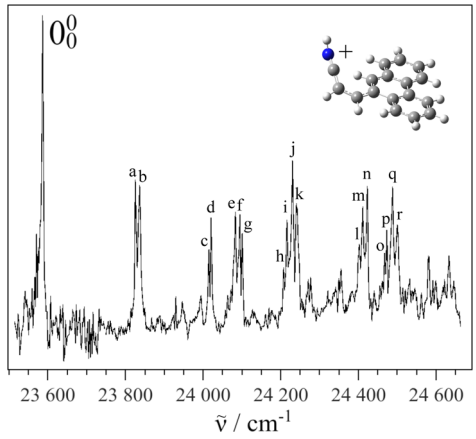

Figure 3. (3) $^1A \leftarrow X\ ^1A$ electronic transition of $C_{17}H_{12}N^+$ recorded with a 0.07 cm^{-1} bandwidth laser. Vibrational bands within the (3) ^1A excited state are listed in Table 3.

3. RESULTS AND DISCUSSION

Protonated azatriphenylene ($1H^+$-1-Azat) was initially considered to be the absorbing species of the three electronic transitions in the visible because of the precursor used in the CI source. Theoretical calculations were performed at the B3LYP/cc-pVDZ level to determine to which atom the additional H is chemically bound. Twelve different protonation sites for 1-azatriphenylene were computed on the ground-state X $^1A'$ potential surface (Table 1); for the lowest-energy isomer of $C_{17}H_{12}N^+$, it is on the nitrogen (Figure 4). The geometries of $C_{17}H_{12}N^+$ were optimized followed by the calculation of the

dx.doi.org/10.1021/jp507616k | J. Phys. Chem. A XXXX, XXX, XXX−XXX

Table 1. Relative Energies of the X $^1A'$ Ground States of Protonated Azatriphenylenes Calculated at the B3LYP/cc-pVDZ Level of Theory and Each Computed Proton Affinity[a]

label	E/kJ mol^{-1}	PA/kJ mol^{-1}	label	E/kJ mol^{-1}	PA/kJ mol^{-1}
1	0	1009	9	151	858
2	181	828	10	146	864
3	154	855	13	134	875
4	197	813	14	148	862
7	151	859	15	137	872
8	147	863	16	142	868

[a]Labelling of the atoms is given in Figure 4.

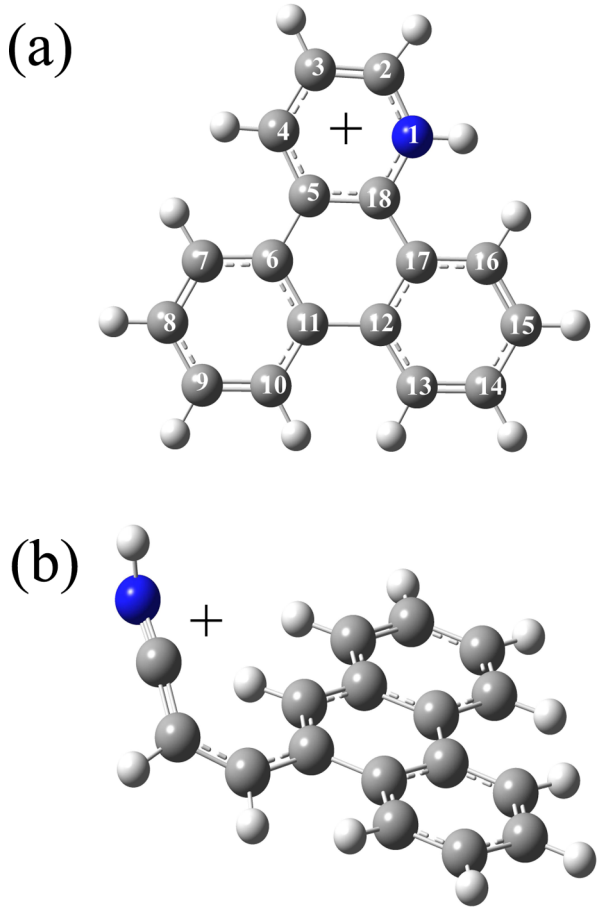

Figure 4. Optimized geometry structure at the B3LYP/cc-pVDZ level of theory of (a) protonated azatriphenylene and (b) the open-ring isomer of $C_{17}H_{12}N^+$.

harmonic frequencies using the three-parameter hybrid density functional theory (DFT) method B3LYP with a double-ζ basis set (cc-pVDZ). Time-dependent DFT (TD-DFT) has been widely used to calculate the electronic transition energy of PAH neutrals, radicals, and ions.[24] Symmetry-adapted cluster/configuration interaction (SAC-CI) was employed to verify consistency with the TD-DFT computations. All calculations were carried out using Gaussian 09.[25] Vertical excitation energies were performed at the B3LYP/cc-pVDZ level for this structure of 1H$^+$-1-Azat; however, as the calculated excitation energies for the electronic transitions differ by >1 eV with the observed spectra, it was concluded that a different isomeric structure was responsible for the absorptions.

The CI source employed can deposit excess energy into 1H$^+$-1-Azat before the ions exit the reaction region. This can dissociate one of the bonds, causing a ring-opening in the conjugated π-system or a loss of a H atom. Therefore, bond cleaving mechanisms, based on the 1H$^+$-1-Azat Mulliken charge distribution, were investigated. Two mechanisms, having the same m/z as 1H$^+$-1-Azat, were considered, one in which the $^{(18)}$C−NH (case 1) bond is broken and the other being between $^{(2)}$C−NH (case 2, Figure 4). In case 1, the geometry of $C_{17}H_{12}N^+$ is that seen in Figure 4b. There is hydrogen migration from $^{(2)}$C to $^{(18)}$C, making a cyanoethyl-substituted phenanthrene. However, in case 2, the calculated structure is not a minimum on the potential energy surface and converges to 1H$^+$-1-Azat. The recorded electronic transitions were finally assigned to the structure shown in Figure 4b because of the good agreement with the theoretical vertical excitation energies. These are 1.92, 2.21, and 3.17 eV for the (3), (2), and (1) ^{1}A ← X ^{1}A electronic transitions, in agreement with the experimental data of 1.80, 2.00, and 2.92 eV (Table 2), the errors being typical for TD-DFT. The theoretical oscillator strengths for the (1) ^{1}A ← X ^{1}A and (2) ^{1}A ← X ^{1}A transitions are approximately 1:6, similar to the relative intensities in the recorded spectrum (Figure 2).

Table 2. Vertical Excitation Energies (eV) Calculated at the SAC-CI and B3LYP Levels of Theory Both with the cc-pVDZ Basis Set for $C_{17}H_{12}N^+$, Phenanthrene with a Cyanoethyl Side Chain

	SAC-CI	B3LYP		
transition	E	E	f	expt.
(1) ^{1}A ← X ^{1}A	1.81	1.92	0.02	1.80
(2) ^{1}A ← X ^{1}A	1.89	2.21	0.13	2.00
(3) ^{1}A ← X ^{1}A	3.20	3.17	0.25	2.92
(4) ^{1}A ← X ^{1}A	4.46	3.54	0.06	
(5) ^{1}A ← X ^{1}A	4.58	3.83	0.01	
(6) ^{1}A ← X ^{1}A	4.68	4.05	0.02	

3.1. (1) ^{1}A ← X ^{1}A Electronic Transition. The (1) ^{1}A ← X ^{1}A electronic transition of $C_{17}H_{12}N^+$ observed in the gas phase has the origin band at 14 519 ± 30 cm^{-1} (Figure 2). Three distinct features are observed in the spectrum at 15 292, 15 509, and 15 721 cm^{-1}, with a similar fwhm as the origin band (158 ± 15 cm^{-1}) and, therefore, belonging to this electronic transition. The (1) ^{1}A excited state lifetime is ∼30 fs, according to the fwhm of the band, because of efficient internal conversion.

3.2. (2) ^{1}A ← X ^{1}A Electronic Transition. A stronger, broader absorption lies ∼1600 cm^{-1} to higher energy of the (1) ^{1}A ← X ^{1}A origin (Figure 2). This feature has a larger fwhm of 307 cm^{-1} compared to the one observed at 14 519 cm^{-1} and is the origin band of the (2) ^{1}A ← X ^{1}A transition. Probably transitions to vibrational levels in the (1) ^{1}A excited state also absorb in this region, mixing the two states and causing a wider, structureless feature to be observed, in addition to fast intramolecular channels. The fwhm of the 0_0^0 band corresponds to a (2) ^{1}A state lifetime of 17 fs.

3.3. (3) ^{1}A ← X ^{1}A Electronic Transition. The (3) ^{1}A ← X ^{1}A electronic transition of $C_{17}H_{12}N^+$ is observed in the 23 500−24 600 cm^{-1} region with an origin band at 23 586 ± 1 cm^{-1} (Figure 3). The 0_0^0 band has a fwhm of 7 cm^{-1}, indicating an excited-state lifetime of ∼750 fs.

dx.doi.org/10.1021/jp507616k | J. Phys. Chem. A XXXX, XXX, XXX−XXX

It is unusual for aromatic systems to have higher excited electronic states undergoing less efficient intramolecular decay, though examples are known, such as azulene. This is also the case for the (3) ^{1}A ← X ^{1}A electronic transition of $C_{17}H_{12}N^+$, where a clear vibrational progression is discernible in the (3) ^{1}A excited state. The next two most intense features (a and b in Figure 3) lie at +239 and +250 cm^{-1} and are assigned to ν_{77} and ν_{76} vibrational modes on the basis of B3LYP/cc-pVDZ calculated frequencies for the X ^{1}A ground state using the double harmonic approximation (Table 3). These are rocking modes of the aromatic rings with a slight movement of the side chain. Band maxima of the (3) ^{1}A excited-state vibrations are listed with suggested assignments in Table 3.

Table 3. Gas-Phase Band Maxima (cm^{-1}) within the Observed (3), (2), and (1) ^{1}A ← X ^{1}A Electronic Transitions of $C_{17}H_{12}N^+$ and Suggested Vibrational Assignment

	$\tilde{\nu}$	$\Delta\tilde{\nu}$	assignment
	14 519	0	0_0^0 (1) ^{1}A ← X ^{1}A
	15 292	773	
	15 509	990	
	15 721	1202	
	16 120	0	0_0^0 (2) ^{1}A ← X ^{1}A
	23 586	0	0_0^0 (3) ^{1}A ← X ^{1}A
a	23 825	239	ν_{77}
b	23 836	250	ν_{76}
c	24 014	428	ν_{71}
d	24 020	434	ν_{70}
e	24 083	497	ν_{68}
f	24 094	508	ν_{66}
g	24 100	514	ν_{65}
h	24 207	621	ν_{62}
i	24 215	629	ν_{61}
j	24 230	644	ν_{60}
k	24 240	654	ν_{59}
l	24 402	816	ν_{52}
m	24 411	825	ν_{51}
n	24 422	836	
o	24 467	881	
p	24 473	887	ν_{50}
q	24 487	901	ν_{49}
r	24 500	914	ν_{48}

4. ASTRONOMICAL CONSIDERATION

As outlined in the Introduction, larger aromatic systems, including nitrogen atoms, are of interest to astronomical observations. The largest linear, unsaturated hydrocarbon containing nitrogen, $HC_{11}N$, was detected in dense interstellar clouds before laboratory microwave data were available.[26,27] Nitrogen has a cosmic abundance approximately that of iron, and thus, molecules comprising one or more N atoms are expected to have a significant population in the ISM. Linear species can undergo cyclization, producing N-containing PAHs given the proper time scale.

Electronic spectra of cations, consisting of 14−50 carbon atoms or including a nitrogen atom, have been previously measured, though not in the gas phase but in an argon matrix.[2,17] These observations were used to improve models for the presence of aromatic species in the ISM. Ionized PANHs have a similar bandwidth for the near-infrared electronic transitions in argon as those reported here for the phenanthrene with a cyanoethyl side chain in the gas phase. Higher excited electronic states were not examined in the matrix studies,[2,17] which could contribute to features in the astronomical spectrum.

The (3), (2), and (1) ^{1}A ← X ^{1}A electronic absorptions of $C_{17}H_{12}N^+$, phenanthrene with a cyano-capped side chain, lie in the visible where DIBs are observed. The bands of the (2) and (1) ^{1}A ← X ^{1}A transitions are much broader (>150 cm^{-1}) than typical DIB widths (∼2 cm^{-1}). In case of the narrower (3) ^{1}A ← X ^{1}A bands, these do not match with known DIBs.[28,29] However, with the approach described, the electronic spectra of even larger aromatic ions can be obtained for an astronomical comparison.

AUTHOR INFORMATION

Corresponding Author

* E-mail: j.p.maier@unibas.ch. Phone: +41 61 267 38 26. Fax: +41 61 267 38 55.

Notes

The authors declare no competing financial interest.

ACKNOWLEDGMENTS

This work was supported by the European Research Council (ERC-AdG-ElecSpecIons:246998) and the Swiss National Science Foundation (Project No. 200020-140316/1).

REFERENCES

(1) Dzhonson, A.; Maier, J. P. Electronic Absorption Spectra of Cold Organic Cations: 2,4-Hexadiyne. *Int. J. Mass Spectrom.* **2006**, *255*−*256*, 139−143.

(2) Mattioda, A. L.; Hudgins, D. M.; Allamandola, L. J. Experimental Near-Infrared Spectroscopy of Polycyclic Aromatic Hydrocarbons between 0.7 and 2.5 μm. *Astrophys. J.* **2005**, *629*, 1188−1210.

(3) Tielens, A. G. G. M. Interstellar Polycyclic Aromatic Hydrocarbon Molecules. *Annu. Rev. Astron. Astrophys.* **2008**, *46*, 289−337.

(4) Hammonds, M.; Pathak, A.; Candian, A.; Sarre, P. J. Spectroscopy of Protonated and Deprotonated PAHs. *EAS Publ. Ser.* **2011**, *46*, 373−379.

(5) Garkusha, I.; Fulara, J.; Sarre, P. J.; Maier, J. P. Electronic Absorption Spectra of Protonated Pyrene and Coronene in Neon Matrixes. *J. Phys. Chem. A* **2011**, *115*, 10972−10978.

(6) Bahou, M.; Wu, Y.-J.; Lee, Y.-P. Infrared Spectra of Protonated Coronene and Its Neutral Counterpart in Solid Parahydrogen: Implications for the Unidentified Interstellar Infrared Emission Bands. *Angew. Chem., Int. Ed.* **2014**, *53*, 1021−1024.

(7) Patzer, A.; Schütz, M.; Jouvet, C.; Dopfer, O. Experimental Observation and Quantum Chemical Characterization of the $S_1 \leftarrow S_0$ Transition of Protonated Naphthalene-Argon Clusters. *J. Phys. Chem. A* **2013**, *117*, 9785−9793.

(8) Knorke, H.; Langer, J.; Oomens, J.; Dopfer, O. Infrared Spectra of Isolated Protonated Polycyclic Aromatic Hydrocarbon Molecules. *Astrophys. J. Lett.* **2009**, *706*, L66−L70.

(9) Krechkivska, O.; Liu, Y.; Lee, K. L. K.; Nauta, K.; Kable, S. H.; Schmidt, T. W. Triple-Resonance Spectroscopy Reveals the Excitation Spectrum of Very Cold, Isomer-Specific Protonated Naphthalene. *J. Phys. Chem. Lett.* **2013**, *4*, 3728−3732.

(10) Hardy, F.-X.; Gause, O.; Rice, C. A.; Maier, J. P. Absorptions in the Visible of Protonated Pyrene Collisionally Cooled to 15 K. *Astrophys. J. Lett.* **2013**, *778*, L30.

(11) Rice, C. A.; Hardy, F.-X.; Gause, O.; Maier, J. P. (1) ^{1}A′−X ^{1}A′ Electronic Transition of Protonated Coronene at 15 K. *J. Phys. Chem. Lett.* **2014**, *5*, 942−945.

(12) Galue, H. A.; Pirali, O.; Oomens, J. Gas-Phase Infrared Spectra of Cationized Nitrogen-Substituted Polycyclic Aromatic Hydrocarbons. *Astron. Astrophys.* **2010**, *517*, A15.

(13) Dryza, V.; Sanelli, J. A.; Robertson, E. G.; Bieske, E. J. Electronic Spectra of Gas-Phase Polycyclic Aromatic Nitrogen Heterocycle Cations: Isoquinoline$^+$ and Quinoline$^+$. *J. Phys. Chem. A* **2012**, *116*, 4323−4329.
(14) Mattioda, A.; Hudgins, D.; Bauschlicher, C.; Rosi, M.; Allamandola, L. Infrared Spectroscopy of Matrix-Isolated Polycyclic Aromatic Compounds and Their Ions. 6. Polycyclic Aromatic Nitrogen Heterocycles. *J. Phys. Chem. A* **2003**, *107*, 1486−1498.
(15) Bernstein, M.; Mattioda, A.; Sandford, S.; Hudgins, D. Laboratory Infrared Spectra of Polycyclic Aromatic Nitrogen Heterocycles: Quinoline and Phenanthridine in Solid Argon and H_2O. *Astrophys. J.* **2005**, *626*, 909−918.
(16) Hudgins, D.; Bauschlicher, C.; Allamandola, L. Variations in the Peak Position of the 6.2 μm Interstellar Emission Feature: A Tracer of N in the Interstellar Polycyclic Aromatic Hydrocarbon Population. *Astrophys. J.* **2005**, *632*, 316−332.
(17) Mattioda, A. L.; Rutter, L.; Parkhill, J.; Head-Gordon, M.; Lee, T. J.; Allamandola, L. J. Near-Infrared Spectroscopy of Nitrogenated Polycyclic Aromatic Hydrocarbon Cations from 0.7 to 2.5 μm. *Astrophys. J.* **2008**, *680*, 1243−1255.
(18) Klærke, B.; Holm, A. I. S.; Andersen, L. H. UV Action Spectroscopy of Protonated PAH Derivatives — Methyl Substituted Quinolines. *Astron. Astrophys.* **2011**, *532*, A132.
(19) Peeters, Z.; Botta, O.; Charnley, S.; Kisiel, Z.; Kuan, Y.; Ehrenfreund, P. Formation and Photostability of N-Heterocycles in Space — I. The Effect of Nitrogen on the Photostability of Small Aromatic Molecules. *Astron. Astrophys.* **2005**, *433*, 583−590.
(20) Soorkia, S.; Taatjes, C. A.; Osborn, D. L.; Selby, T. M.; Trevitt, A. J.; Wilson, K. R.; Leone, S. R. Direct Detection of Pyridine Formation by the Reaction of CH(CD) with Pyrrole: A Ring Expansion Reaction. *Phys. Chem. Chem. Phys.* **2010**, *12*, 8750−8758.
(21) Elsila, J. E.; Hammond, M. R.; Bernstein, M. P.; Sandford, S. A.; Zare, R. N. UV Photolysis of Quinoline in Interstellar Ice Analogs. *Meteorit. Planet. Sci.* **2006**, *41*, 785−796.
(22) Gerlich, D. Inhomogeneous RF Fields: A Versatile Tool for the Study of Processes with Slow Ions. *Adv. Chem. Phys.* **1992**, *82*, 1−176.
(23) Gerlich, D. Ion-Neutral Collisions in a 22-Pole Trap at Very Low Energies. *Phys. Scr.* **1995**, *T59*, 256−263.
(24) Hammonds, M.; Pathak, A.; Sarre, P. J. TD-DFT Calculations of Electronic Spectra of Hydrogenated Protonated Polycyclic Aromatic Hydrocarbon (PAH) Molecules: Implications for the Origin of the Diffuse Interstellar Bands? *Phys. Chem. Chem. Phys.* **2009**, *11*, 4458−4464.
(25) Frisch, M. J.; Trucks, G. W.; Schlegel, H. B.; Scuseria, G. E.; Robb, M. A.; Cheeseman, J. R.; Scalmani, G.; Barone, V.; Mennucci, B.; Petersson, G. A.; et al. *Gaussian 09*, revision D.01; Gaussian Inc.: Wallingford, CT, 2009.
(26) Oka, T. The Prediction of the Rotational Constants of Polyacetylene Compounds H−(C≡C)$_n$−C≡N. *J. Mol. Spectrosc.* **1978**, *72*, 172−174.
(27) Bell, M. B.; Feldman, P. A.; Travers, M. J.; McCarthy, M. C.; Gottlieb, C. A.; Thaddeus, P. Detection of $HC_{11}N$ in the Cold Dust Cloud TMC-1. *Astrophys. J. Lett.* **1997**, *483*, L61.
(28) Hobbs, L. M.; York, D. G.; Snow, T. P.; Oka, T.; Thorburn, J. A.; Bishof, M.; Friedman, S. D.; McCall, B. J.; Rachford, B.; Sonnentrucker, P.; et al. A Catalog of Diffuse Interstellar Bands in the Spectrum of HD 204827. *Astrophys. J.* **2008**, *680*, 1256−1270.
(29) Hobbs, L. M.; York, D. G.; Thorburn, J. A.; Snow, T. P.; Bishof, M.; Friedman, S. D.; McCall, B. J.; Oka, T.; Rachford, B.; Sonnentrucker, P.; et al. Studies of the Diffuse Interstellar Bands. III. HD 183143. *Astrophys. J.* **2009**, *705*, 32−45.